Structure and function of the endothelial glycocalyx in the microcirculation

Dane, M.J.C.

5

Association of kidney function with changes in the endothelial surface layer

CJASN 9: 698-704, 2014

Martijn J.C. Dane[1,3], Meriem Khairoun[1], Dae Hyun Lee[1], Bernard M. van den Berg[1], Bart J.M. Eskens[2], Margien G.S. Boels[1], Jurgen W.G.E. van Teeffelen[2], Angelique L.W.M.M. Rops[3], Johan van der Vlag[3], Anton Jan van Zonneveld[1], Marlies E.J. Reinders[1], Hans Vink[2], Ton J. Rabelink[1]

[1]Department of Nephrology, Einthoven laboratory for Vascular Medicine, Leiden University Medical Center, the Netherlands [2]Department of Physiology, Maastricht University Medical Center, Maastricht, the Netherlands [3]Department of Nephrology, Nijmegen Center for Molecular Life Sciences, Radboud University Nijmegen Medical Center, Nijmegen, the Netherlands

Abstract

End-stage renal disease (ESRD) is accompanied by endothelial dysfunction. Since the endothelial glycocalyx (endothelial surface layer, ESL) governs interactions between flowing blood and the vessel wall, perturbation could influence disease progression. In this study we used a novel non-invasive sidestream-darkfield (SDF) imaging method, which measures the accessibility of red blood cells to the ESL in the microcirculation (perfused boundary region, PBR), to investigate whether renal function is associated with ESL dimensions. PBR was measured in control participants (n=10), in patients with ESRD (n=23), in participants that have normal kidney function after successful living donor kidney transplantation (n=12) and in patients who developed interstitial fibrosis / tubular atrophy after kidney transplantation (n=10). In addition, the endothelial activation marker Angiopoietin-2 (Ang2) and shed ESL components syndecan-1 and soluble thrombomodulin (sTM) were measured using ELISA. Compared to healthy controls (1.82±0.16 μm), ESRD patients had a larger PBR (+0.23, [95%CI, 0.459 to 0.003], P<0.05), which signifies loss of ESL dimensions. This large PBR was accompanied by higher circulating levels of syndecan-1 (+57.71 [CI95%, 17.38 to 98.04] p<0.01) and sTM (+12.88 [95%CI, 0.29 to 25.46], p<0.001). After successful transplantation, the PBR was indistinguishable from healthy controls, without elevated levels of sTM or syndecan-1. In contrast however, patients who developed IFTA showed a large PBR (+0.36 [95%CI, 0.09 to 0.63]; p<0.01) and higher levels of endothelial activation markers. In addition, a significant correlation between PBR, Ang2 and eGFR was observed (PBR vs. GFR: spearman's rho 0.31 p<0.05 and PBR vs. Ang2: spearman's rho -0.33 p<0.05).
In this study we have shown that reduced renal function is strongly associated with low ESL dimensions. After successful kidney transplantation the ESL is indistinguishable from control.. Our new SDF-based method allows rapid and unbiased assessment of these ESL dimensions in clinical medicine.

Introduction

Patients with end stage renal disease (ESRD) have a dysfunctional endothelium and increased morbidity and mortality, mainly due to their increased risk for cardiovascular disease [1,2]. The mechanisms responsible for activation of the endothelium in chronic renal failure are multifactorial and include the presence of uremic toxins (in particular asymmetric dimethyl arginine), low grade inflammation, and hypertension [3]. One of the earliest changes upon this endothelial activation has been postulated to be compositional- and dimensional alterations of the endothelial surface layer (ESL) [4].

The ESL is a carbohydrate gel-like layer composed of proteoglycans, glycoproteins and loosely bound plasma molecules [5-7]. It has been postulated to govern the interaction between blood and the vessel wall. Heparan sulfates, the main constituent of the ESL, have been shown to activate antithrombin III and to prevent leucocyte interaction with the endothelium [8-11]. In addition, the ESL regulates endothelial permeability and acts as shear stress sensor in the control of vasomotor function [12,13]. It is therefore very likely that alterations in, or loss of, ESL function can predispose for the development of vascular disease [14,15]. Under inflammatory conditions the ESL induces changes in surface heparan sulfate composition that facilitate the recruitment of inflammatory cells [14]. With sustained inflammation, the production of heparanase is induced in the glomerulus, which may partially degrade the ESL. Prevention of this ESL loss in diabetic heparanase knock-out mice also prevented the development of proteinuria and kidney injury [16]. Thus, ESL function and dimensions are also an important determinant of progression of kidney disease.

Because the ESL is being produced and shed continuously and its dimensions are, among others, based on blood pressure and plasma proteins, it is very challenging to analyze [5-7]. Most methods that aim to detect changes in ESL are based on the measurement of shed ESL components like proteoglycans, hyaluronan or heparan sulfates in the plasma. The only direct measurements for ESL properties are currently done in animals only, using perfusion-staining or intra-vital techniques [13,17,18]. Until recently, ESL changes were measured using an invasive and time consuming method, by using the distribution of labeled red blood cells (RBC) and low molecular weight dextrans [19]. Recently, a non-invasive tool for analyzing the ESL was developed using sidestream-darkfield (SDF) imaging. ESL dimensions were calculated as the difference in RBC column width before (functionally perfused capillary diameter) and after (anatomical capillary diameter) leukocyte passage. This technology correlates well with the invasive techniques based on tracer dilution to assess the volume of the ESL, which is very labor intensive and subject to investigator bias [20]. We use a new approach in which spatiotemporal changes in the ability of RBCs to penetrate the ESL can be detected [21]. This method is fully automated and blinded to the investigator. In contrast to previous methods, in which the ESL quantity was measured in volume or thickness, this method analyses ESL quality: a larger PBR, or increased accessibility to RBCs, reflects a disturbance of the ESL structure.

In the present study we utilized this method to investigate the hypothesis that renal failure is associated with perturbation of the endothelial ESL, i.e. larger PBR, and its relation to the presence of shed ESL components syndecan-1 and thrombomodulin (sTM) and the endothelial activation marker angiopoietin-2 (Ang2). In addition we measured the ESL in patients who received kidney transplantation.

Material and methods

Study population

In a previous study, endothelial function has been shown to be estrogen-dependent and thus varies during the menstrual cycle [22]. Furthermore, in a currently on-going study we could demonstrate a small but significant difference in baseline PBR between man and woman (unpublished data). As the exact reason of these differences is still unclear, we only studied male participants in the current study to exclude gender as a possible confounding factor. A total of 53 male patients and 10 age-matched male controls were enrolled in a cross-sectional study in which PBR was measured (table 1). 31 Patients were included after being diagnosed with ESRD (eGFR<15 mL/min/1.73 m2), 12 with stable renal function after kidney transplantation (eGFR=30mL/min/1.73 m2 or higher or more, stable group) and 10 with interstitial fibrosis and tubular atrophy (IFTA) developed after kidney transplantation, (eGFR<30mL/min/1.73 m2or less and histopathologic proof, IFTA group). This latter group was included to investigate whether loss of function of the transplanted kidney would result in perturbation of the ESL. All procedures were approved by the Leiden University Medical Center (LUMC) institution's Medical Ethical Committee and complied with the declaration of Helsinki's guidelines. Informed consent was obtained from all patients.

Transplantation

All patients received kidney transplantation at the LUMC between 1984 and 2012. Transplantations were performed as described previously [23]. Patients were treated with prednisone (tapered to a dose of 10 mg by 6 weeks and a dose of 5-7.5 mg by 3 months), cyclosporine (area under the curve (AUC) 5400 ng.h/mL first 6 weeks then 3250 ng.h/mL) or tacrolimus (AUC 210 ng.h/mL first 6 weeks, then 125 ng.h/mL) and mycophenolate mofetil (MMF) (AUC 30-60 ng.h/mL). From the year 2000 on, these patients received induction treatment with basiliximab (40 mg at day 0 and 4) or daclizumab (100 mg/day on the day of transplantation and 10 days after transplantation). Patients were treated routinely with oral val-ganciclovir profylaxis for 3 months, except for a CMV negative donor recipient status. The clinical and research activities being reported are consistent with the Principles of the Declaration of Istanbul as outlined in the 'Declaration of Istanbul on Organ Trafficking and Transplant Tourism.

Imaging of the sublingual microvasculature

Imaging of microcirculation: To detect the dynamic lateral RBC movement into the glycocalyx of the microcirculation (expressed as PBR), sidestream dark field (SDF) intravital microscopy (MicroVision Medical Inc., Wallingford, PA) [24] was performed to visualize the sublingual microvasculature. The method of calculation is based on the method published before and is fully automated to ensure unbiased analysis of the ESL [21]. The SDF camera uses green light emitting diodes (540nm) to detect the haemoglobin of passing RBC. The images were captured using a 5x objective with a 0.2 NA (numerical aperture), providing a 325- fold magnification in 720 x 576 pixels at 23 frames per second.

The image acquisition is automatically mediated through the Glycocheck software (Glycocheck BV, Maastricht, the Netherlands). With this method it is possible to detect increased penetration of RBCs into the glycocalyx (increased PBR) when the glycocalyx is perturbed or degraded.
Calculating the PBR: The software automatically identifies all available measurable microvessels, in focus and without movement of the imaging unit and defines vascular segments every 10μm along the length of these vessels (**figure 1A,B**). Subsequently, a sequence of 40 frames is recorded in time, containing on average 300 vascular segments. Then the observer moves the SDF imaging unit to a different location for another recording session of 40 frames, until a total of minimal 3,000 vascular segments are recorded. After these measurements, 21 line markers are placed at an interval of 0.5μm around all vascular segments (**figure 1C,D**).

From these line markers in the recorded movies, the PBR is calculated. First, the width of the red blood cell column is measured by determining both inflection points of the intensity plot profiles of all line markers (**figure 1E**). This results in 840 red blood cell column widths per vascular segment (21 line markers * 40 frames). Second, for every vascular segment, the measurements of all these RBC column widths are combined into a graph as shown in **figure 1F**. The number of observed RBC positions (as a percentage of the total) is plotted against the measured column width. From this graph the median column width is derived, being the 50th percentile of the curve. By linear regression analysis, the slope of the line between the 25th and the 75th percentile is measured. The point where this line intersects with the x-axis is a reliable marker (based on all 840 measurements) of the most outward location of the RBC, the perfused diameter (PD).

The PBR is defined as the distance between RBC column width and PD. Because the PBR is present on both sides of the RBC column, it is calculated using the equation: [PD – median RBC column width] / 2. The calculated PBR values, classified according to their corresponding RBC column width between 5 – 25 μm, are averaged to provide a single PBR value for each participant. Finally, the PBR is schematically shown in **figure 1G**.

Quality checks: To ensure a reliable and reproducible measurement quality checks are performed during the whole analysis procedure. First, the software only selects the vascular segments of which at least 11 of the 21 line markers have a positive signal for the presence of an RBC (>50% of the vascular segment is filled with RBCs) to use for the subsequent analyses from the first frame of the different recordings. By selecting only the vascular segments that are filled for more than 50%, the influence of hematocrit on the PBR measurements is minimized.

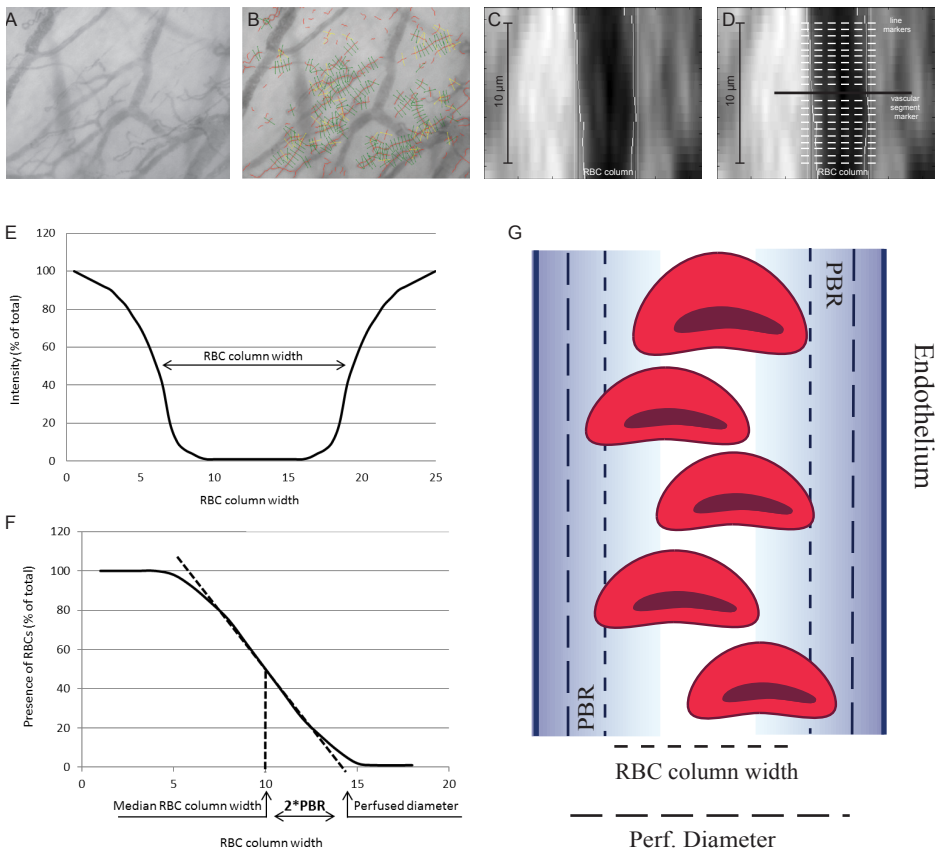

Figure 1: Image acquisition and logarithm to calculate PBR in sublingual microvasculature.
A: Example of one frame made using the SDF camera. The camera detects the haemoglobin of passing RBCs by green light emitting diodes (540nm) and the software automatically identifies all available measurable micro-vessels in focus. B: Example of the same frame of the acquired image after vascular segments have been defined every 10µm along the length of these vessels, until at least 3000 vascular segments are recorded. C: Zoomed in example of one vascular segment of the RBC column. D. Schematic example with the vascular segment marker and the 21 line markers on and around the vascular segment marker. E. Example of a plot profile of the RBC column width measured at one line marker. F: Graph of all RBC column widths measured at one vascular segment. From this plot the median RBC column width can be calculated. The perfused diameter can be determined by using linear regression on the area of the curve from the 25th to the 75th percentile. Next the PBR can be calculated from these two parameters. G: Schematic image of cross section of a blood vessel with the RBC column width, perfused diameter and PBR explained.

The second quality check is performed during the measurement of all RBC column widths (figure S1E). In the second quality check all measured segments are tested on minimal RBC width-, position of the column (centred or not) and the signal to noise ratio. In the third quality check the curve fit for calculating the median RBC column width and PD is tested (R2 of 25th to 75th percentile > 0.75) (figure S1F). Measurement points that do not fulfil the criteria of these quality checks are not used for the calculation of the PBR.

Validation of the SDF method

To validate the measurements, a direct test to determine whether loss of glycocalyx dimension is reflected by outward radial displacement of circulating RBCs has been performed using intravital microscopy. For this experiment, B6.Cg-Tg(TIE2GFP)287Sato/1J mice were used (Jackson Laboratories, Bar Harbor, ME). In these mice endothelial cells (EC) can be imaged by the specific expression of GFP in ECs. These GFP-EC mice were prepared for intravital microscopic observation of the cremasteric microcirculation as described before.[25] The preparation was transferred to the stage of an intravital microscope (Leitz, Wetzlar, Germany), coupled to a cooled CCD video camera (C9100; Hamamatsu, Hamamatsu City, Japan). Microvessels were alternately observed using bright-field microscopy with a 435 nm band pass interference filter (blue light) in the light path for depiction of the RBC column and epi-illumination for examination of the GFP signal using the appropriate filters for fluorescein. A salt water immersion objective lens (x50, n.a. 1.0) was used. From these two images from the same microvessel segment (figure S2), the anatomic vessel width was determined using the endothelial position by the GFP intensity peak while the perfused diameter was determined by the width of the RBC profile at half height intensity. The RBC-EC gap, or the space between endothelial cell and RBC column, is calculated from the difference between vessel diameter and corresponding perfused diameter, divided by two (as the gap is present on both sides of the RBC column). To determine the effect of glycocalyx degradation on the outward displacement of the RBC column, paired measurements in a total 16 vessels in 7 mice have been performed before and 30 minutes after hyaluronidase treatment (35 U, jugular vein infusion).

Laboratory and urinary assessments

All persons enrolled in this study underwent blood sampling before the morning intake of immunosuppression. Creatinine, hematocrit and hemoglobin were measured. For all patients the eGFR was calculated from the plasma creatinine concentration using the Modification of Diet in Renal Disease (MDRD) formula. Simultaneously, blood was collected for analysis of Ang2 and sTM in serum and syndecan-1 in plasma. Ang2 (ELISA; R&D Systems, Minneapolis, MN, USA), sTM and syndecan-1 (ELISA; Diaclone Research, Besancon, France) concentrations were measured by their respective enzyme-linked immunosorbent assay according to the protocol supplied by the manufacturer.

Statistical analyses

Continuous normally distributed data are presented as mean ± SD, unless stated otherwise. Differences between the groups were tested by analysis of variance (ANOVA) and shown

as (difference compared to control [95% confidence interval], p-value). When criteria for parametric testing were not met, median and interquartile range (IQR) are presented and tested with the Mann-Whitney test. Correlations between interval variables were calculated using the Spearman rank correlation coefficient. Differences were considered statistically significant if $p<0.05$. Data analysis was performed using SPSS version 20.0 (SPSS Inc, Chicago, IL) and GraphPad Prism, version 5.0 (GraphPad Prism Software Inc, San Diego, CA).

Results

Method validation in mice

To validate the PBR measurements, the gap between endothelial cells and RBC column (RBC-EC gap) was measured in mice before and 30 minutes after i.v. administration of the glycocalyx degrading enzyme hyaluronidase (supplemental methods). RBC-EC gaps ranged from 0.3 – 2.6 microns (vessel diameters 5 – 35 microns). Hyaluronidase treatment reduced the RBC-EC gap from 1.30 to 0.52 microns (average vessel diameter 16.0 microns) (**figure 2**). To exclude that changes in the RBC-EC gap originate from changes in the vessel diameter, the vessel diameter was measured before and after hyaluronidase treatment (**figure 2**). Because no changes could be observed in these paired measurements (p=0.91) the influence of vessel diameter can be excluded, thereby confirming that the observed changes originate from the changes in RBC column size as a result of the degradation of the ESL.

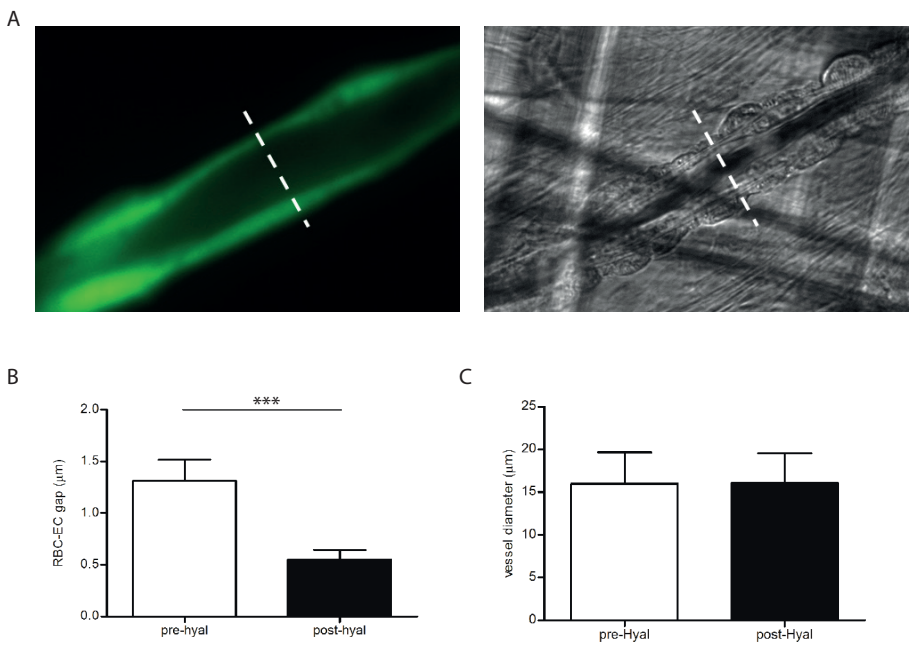

Figure 2: Validating the method in hyaluronidase treated mice. *A: Example of the epifluorescence- (GFP, green) and trans-illumination (RBC, black) images made for measurement of both the vessel width using the endothelial cell GFP signal and the perfused diameter using the RBC column width. B: Paired measurements of changes in EC-RBC gap before and after hyaluronidase treatment. (*** P<0,001) C: Paired measurements of changes in vessel diameter before and after hyaluronidase treatment show no differences.*

Patient Characteristics

Clinical characteristics of all patients included in this study are described in table 1. No differences were observed in age, blood pressure or BMI. The eGFR, was significantly lower in all patient groups compared to controls ($p<0.05$). Hemoglobin and mean corpuscular volume (MCV) levels were significantly lower in patients with ESRD and IFTA compared to controls (**table 1**) ($P<0.05$).

Comparison of ESL among patient groups

Changes in ESL related to endothelial activation are hypothesized to be one of the first changes in the development of cardiovascular disease [4,14]. Therefore; we measured the distance in which the RBCs can penetrate the ESL of which the calculated PBR reflects the ESL barrier properties. In this study, the PBR in controls was comparable to the PBR measured in controls in an earlier published study with lacunar stroke patients [21]. Compared to healthy controls (1.82±0.16 μm), the PBR in patients with ESRD was significantly different (+0.23, [95%CI, 0.459 to 0.003], $P<0.05$). Patients who developed IFTA also showed a different PBR (+0.36 [95%CI, 0.09 to 0.63]; $p<0.01$). Interestingly, the PBR in stable transplanted participants was larger, but statistically indistinguishable from healthy controls (1.85±0.20 μm, $p=1$) (**Figure 3**). To determine the influence of dialysis on the PBR, we compared patients who received dialysis (n=9) with patients without dialysis (n=14) within the ESRD group. No difference was observed between these patient groups (2.02±0.21 vs. 2.07±0.29 μm respectively, $p=0.62$), which suggest that dialysis does not contribute to the observed differences in PBR (**Figure 4**).

Characteristic	control (n=10)	ESRD (n=23)	Stable (n=12)	IFTA (n=10)
Age (yrs)	44.8 (±10.3)	50.6 (±12.4)	54.1 (±13.9)	56.0 (±9.4)
Smoking, N (%)	0	1	2 (17%)	2 (20%)
Time since Tx (median years) (IQR)	-	-	5.0 (1.0-7.5)	8.0 (3.0-14.5)
BMI (kg/m²)	25.6 (±3.7)	25.92 (±4.1)	26.2 (±3.4)	23.8 (±3.0)
eGFR (ml/min/1,73 m²)	86.8 (± 17.2)	8.2 (± 2.7)*	61.2 (±16.8)*	22.3 (±9.03)*
Systolic BP (mmHg)	132.8 (±11.6)	139.5 (±12.9)	132.4 (±9.1)	141.9 (±20.5)
Diastolic BP (mmHg)	80.6 (±7.1)	83.0 (±12.54)	78.1 (±6.2)	81.5 (±6.9)
Hemoglobin (mmol/L)	9.25 (±0.45)	7.71 (±1.00)*	8.96 (±1.24)	7.17 (±1.18)*
Hematocrit (L/L)	0.43 (±0.03)	0.38 (± 0.05)	0.44 (±0.05)	0.37 (±0.05)*
MCV (fL)	88.8 (±2.6)	92.9 (±4.1)	89.7 (±3.4)	95.4 (± 5.5)*
Median proteinuria (g/24hr) (I.Q.R)	-	2.04 (±1.81)	0.23 (±0.10)	2.27 (±2.38)
Anti-coagulation, N (%)	-	5 (22%)	0 (0%)	6 (60%)
Anti-hypertensives, N (%)	-	23 (100%)	8 (67%)	10 (100%)
Statins, N (%)	-	12 (52%)	2 (17%)	6 (60%)
Immunosuppressives, N (%)	-	4 (17%)	12 (100%)	10 (100%)

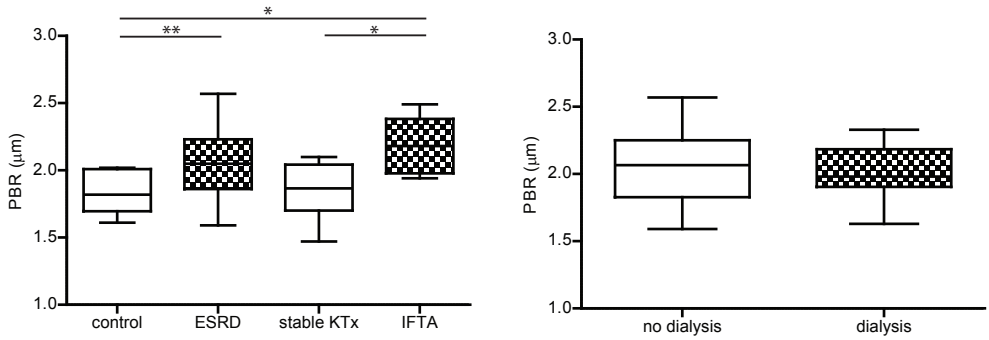

Figure 3: Measurements of the perfused boundary region in participants with and without loss of renal function. *PBR in healthy control participants (control, n=10), and in patients diagnosed with end stage renal disease (ESRD, n=23), stable kidney transplantation (stable KTx, n=12) and interstitial fibrosis and tubular atrophy (IFTA, n=10). Box-plot whiskers indicate 1st and 99th percentile. *P<0.05, **P<0.01*

Figure 4: Measurements of the perfused boundary region in ESRD patients with and without dialysis*. PBR in patient who did receive dialysis (n=9), and in patients who did not receive dialyis (n=14), within the ESRD group. Box-plot whiskers indicate 1st and 99th percentile.*

The endothelial activation state was determined by measuring serum Ang2 levels. In agreement with increasing PBR, the Ang2 level was higher, although not significant, compared to control levels (4.21±3.23 and 2.09±1.16 ng/mL, p=0.19) in ESRD serum samples (**figure 5a**). There was no difference in Ang2 levels in the successfully transplanted or the IFTA group (1.68±0.85 and 3.59±2.34 ng/mL, both p=1). Next, markers of shed ESL compounds were measured. Serum sTM levels between control participants (7.06±1.17 ng/mL) and ESRD patients were significantly different (+12.88 [95%CI, 0.29 to 25.46], p<0.001). Patients diagnosed with IFTA had even higher serum sTM levels (+34.86 [95%CI 19.87 to 49.86], p<0.001). In participants with a stable KTx, sTM levels were indistinguishable from control (12.98±3.01 ng/mL, p=1) (**figure 5b**). In accordance, shed syndecan-1 levels were high compared to control (49.8 ±17.4 ng/mL) in ESRD patients (+57.71 [CI95%, 17.38 to 98.04] p<0.01). However, shed syndecan-1 levels were not significantly different from controls in both IFTA and stable KTx samples (54.8±32.7 and 64.0±15.2 ng/mL, respectively) (**figure 5c**).

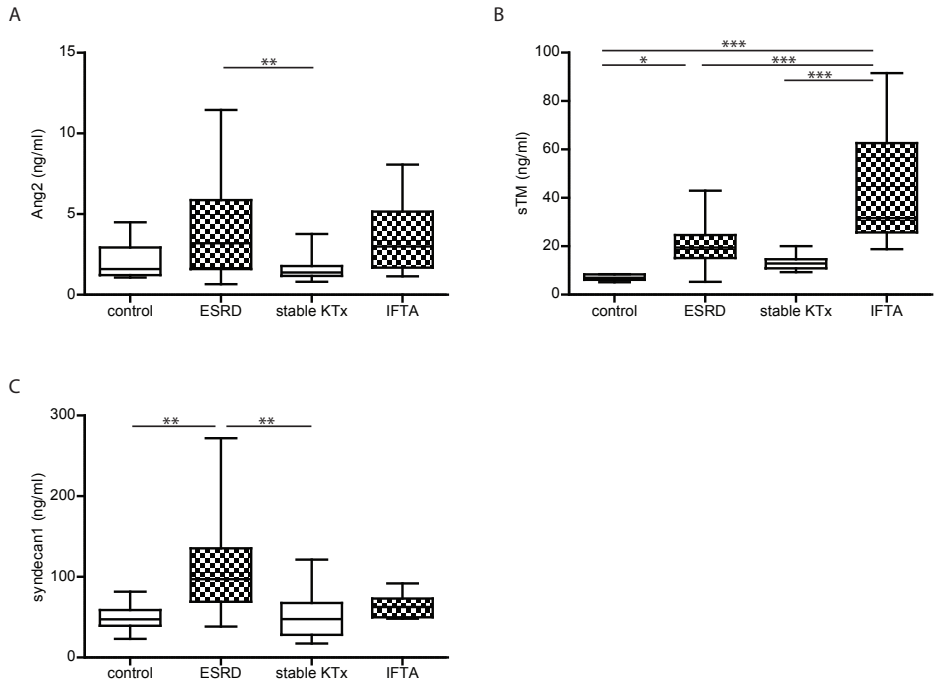

Figure 5: Measurements of circulatory endothelial and ESL damage markers in participants with- and without loss of renal function. *Markers were measured in healthy control participants (control, n=10), and in patients diagnosed with end stage renal disease (ESRD, n=23), stable kidney transplantation (stable KTx, n=12) and interstitial fibrosis and tubular atrophy (IFTA, n=10). A: serum Angiopoietin2 B: serum sTM and C: plasma shed syndecan-1. Box-plot whiskers indicate 1st and 99th percentile. *P<0.05, **P<0.01 **P<0.001*

To examine any relation between renal failure, health status of the microcirculation and ESL composition, the following correlations were achieved (**table 2**). Firstly, the endothelial cell activation marker Ang2 inversely correlated with renal function, as assessed by the eGFR (Spearman's rho=-0.40, p<0.01), suggesting a relation between endothelial dysfunction and renal failure. Similarly, PBR was inversely correlated with the eGFR (Spearman's rho = -0.33, p<0.05) and positively correlated with serum Ang2 levels (Spearman's rho = 0.31, p<0.05). A comparable inverse correlation of sTM and syndecan-1 with eGFR (Spearman's rho = -0.53 and -0.67, respectively; both p<0.001) supports the indication that endothelial activation and a perturbed ESL are associated with global renal function.

Association between PBR and shed endothelial surface layer markers

Since both PBR and shed ESL markers associated with the observed differences in renal function, we tested the possible relation between the endothelial surface markers (**table 2**). Although we were able to find a positive correlation between PBR and sTM (Spearman's rho=0.33, p<0.05) and between sTM and shed syndecan-1 (Spearman's rho=0.45, p<0.001), no significant correlation between PBR and shed syndecan-1 was found (spearman's rho=0.13 p=0.35).

		eGFR (ml/min/1,73 m^2)	PBR (µm)
PBR	**Spearman's rho**	-0.33	-
		P<0.05	-
Ang2	**Spearman's rho**	-0.40	0.31
		P<0.01	P<0.05
sTM	**Spearman's rho**	-0.57	0.33
		P<0.001	P<0.05
Syndecan-1	**Spearman's rho**	-0.67	0.13
		P<0.001	P=0.35

Discussion

We show that patients with impaired kidney function have a larger PBR, i.e. loss of endothelial surface layer. Interestingly, ESL dimensions in patients with a stable kidney transplant were indistinguishable from healthy controls, while loss of renal function in patients developing IFTA resulted again in perturbation of the ESL. These changes in PBR are reflected by the presence of circulating ESL components, sTM and syndecan-1.

In the current study we used a new non-invasive, automated, and easy to apply approach to measure the ability of RBC to penetrate the ESL, quantitatively defined as the perfused boundary region. The automated software analysis results in an average PBR of 1.82μm in healthy control participants, which is lower than the previously published PBR of 3.3μm [26], but far more reliable because this new method uses over 3000 measurement sites and stringently removes artifacts and background signal. Moreover, it ensures unbiased data analysis.

Ang2 is released by endothelial cells upon their activation [27,28]. The paracrine release of Ang2 interferes with Ang1 signaling from perivascular cells towards the endothelium, resulting in capillary destabilization and angiogenic responses [29,30]. The correlation we show between Ang2, eGFR and PBR indicates that the endothelial activation during renal failure is associated with a loss of ESL dimensions.

TM, is an anticoagulant cell surface proteoglycan which is shed from the endothelial cell surface layer after inflammatory stimulation, resulting in the soluble TM we measured in serum [31]. Although it is also expressed in low amounts by dendritic cells and monocytes, it is mainly expressed by endothelial cells, thereby making it a reasonable marker for shedding of proteoglycans from the ESL. In this study we show a negative correlation between serum sTM and renal function (eGFR), which has also been shown in type 1 diabetic patients after simultaneous pancreas–kidney transplantation [23]. Although shedding from the ESL most likely explains higher sTM, reduced clearance by the kidneys needs to be considered as well. A study in diabetic patients, however, showed that urinary sTM was not influenced by GFR [32]. Also the size of sTM would preclude filtration by the kidney. Together, these data indicate that the high levels of sTM are a direct result of increased TM shedding from the ESL.

In addition to TM, syndecan-1 is also shown to be expressed at the luminal endothelial surface [33,34]. Its shedding from the ESL under inflammatory conditions is thought to contribute to plasma levels of soluble syndecan-1 [35]. In agreement, syndecan-1 shedding has been shown previously to be associated with ischemia-reperfusion injury, septic shock and post cardiac arrest syndrome [33,36,37]. In addition, patients with early diabetic nephropathy have higher shed syndecan-1 levels compared to healthy controls [38]. Alternatively, reduced renal clearance of syndecan-1 could as well be involved in elevated plasma levels in patients with renal failure. While little is known about the exact

clearance mechanism of syndecan-1, its large molecular weight excludes a direct straight forward relationship with GFR. Although the large PBR and sTM levels coincided with high syndecan-1 levels in ESRD patients, transplant recipients with IFTA and reduced renal function still showed low levels of syndecan-1.

Interestingly, in patients who were stable after kidney transplantation, sTM and PBR was not similar, but also not significantly different from the measured PBR in ESRD patients or the healthy controls. This position in between healthy controls and ESRD patients might be explained by the fact that kidney function is still not optimal compared to healthy controls. The higher level of sTM in IFTA patients compared to ESRD patients is absent for syndecan-1, which suggests that the various pathologies that underlie renal failure in these patients affect the shedding of ESL components differently.

All together, the plasma and serum biomarkers and PBR measurements corroborate the observation that loss of renal function is associated with endothelial activation and ensuing loss of ESL thickness. A question is whether mucosal ESL thickness is representative for systemic changes. However, as with other endothelial function measurements, systemic factors will induce representative functional endothelial changes throughout the circulation. Using dextran distribution we previously validated in patients with diabetes that such mucosal changes in ESL thickness are indeed accompanied by changes in systemic ESL thickness [39]. In addition, ESL changes have also been shown to coincide in both the retinal and the sublingual microcirculation in patients with type 2 diabetes [40].

In this study we cannot completely exclude the effect of immunosuppression in the transplant patients on the mechanical properties of the ESL. Nonetheless, a clear change in PBR was observed between the kidney recipients with stable function versus the IFTA group, while both groups were treated with immunosuppressive medication, suggesting that renal function per se is a more important determinant of PBR. Another question is whether changes in RBC deformability may have contributed to the observed PBR measurements. A study by Martinez et al did not observe any alteration in erythrocyte deformability between control participants and patients with CKD with or without dialysis, which makes a contribution of RBC deformability to the observed differences in PBR less likely for these patients [41].

Changes in the ESL have been postulated to precede vascular (and renal) damage [4]. Because measuring PBR in the microcirculation is a non-invasive and fast method to assess changes in the ESL in patients, this is a promising new method for clinical monitoring of the systemic microvasculature to predict the risk for cardiovascular disease and to follow the vascular effect of interventions, such as kidney transplantation.

Acknowledgements
The study was supported by the Dutch Kidney Foundation (grant number C08.2265 and the Glycoren consortium grant CP09.03)

References

1. Santoro D, Bellinghieri G, Conti G, Pazzano D, Satta E, et al. (2010) Endothelial dysfunction in chronic renal failure. J Ren Nutr 20: S103-108.
2. Schiffrin EL, Lipman ML, Mann JF (2007) Chronic kidney disease: effects on the cardiovascular system. Circulation 116: 85-97.
3. Moody WE, Edwards NC, Madhani M, Chue CD, Steeds RP, et al. (2012) Endothelial dysfunction and cardiovascular disease in early-stage chronic kidney disease: cause or association? Atherosclerosis 223: 86-94.
4. Rabelink TJ, de Boer HC, van Zonneveld AJ (2010) Endothelial activation and circulating markers of endothelial activation in kidney disease. Nat Rev Nephrol 6: 404-414.
5. Reitsma S, Slaaf DW, Vink H, van Zandvoort MA, oude Egbrink MG (2007) The endothelial glycocalyx: composition, functions, and visualization. Pflugers Arch 454: 345-359.
6. Weinbaum S, Tarbell JM, Damiano ER (2007) The structure and function of the endothelial glycocalyx layer. Annu Rev Biomed Eng 9: 121-167.
7. Pries AR, Secomb TW, Gaehtgens P (2000) The endothelial surface layer. Pflugers Arch 440:653-666.
8. Boels MG, Lee DH, van den Berg BM, Dane MJ, van der Vlag J, et al. (2013) The endothelial glycocalyx as a potential modifier of the hemolytic uremic syndrome. Eur J Intern Med.
9. Mertens G, Cassiman JJ, Van den Berghe H, Vermylen J, David G (1992) Cell surface heparan sulfate proteoglycans from human vascular endothelial cells. Core protein characterization and antithrombin III binding properties. J Biol Chem 267: 20435-20443.
10. Rops AL, van den Hoven MJ, Baselmans MM, Lensen JF, Wijnhoven TJ, et al. (2008) Heparan sulfate domains on cultured activated glomerular endothelial cells mediate leukocyte trafficking. Kidney Int 73: 52-62.
11. Constantinescu AA, Vink H, Spaan JA (2003) Endothelial cell glycocalyx modulates immobilization of leukocytes at the endothelial surface. Arterioscler Thromb Vasc Biol 23:1541-1547.
12. Weinbaum S, Zhang X, Han Y, Vink H, Cowin SC (2003) Mechanotransduction and flow across the endothelial glycocalyx. Proc Natl Acad Sci U S A 100: 7988-7995.
13. Dane MJ, van den Berg BM, Avramut MC, Faas FG, van der Vlag J, et al. (2013) Glomerular Endothelial Surface Layer Acts as a Barrier against Albumin Filtration. Am J Pathol 182: 1532-1540.
14. Becker BF, Chappell D, Bruegger D, Annecke T, Jacob M (2010) Therapeutic strategies targeting the endothelial glycocalyx: acute deficits, but great potential. Cardiovasc Res 87:300-310.
15. Broekhuizen LN, Mooij HL, Kastelein JJ, Stroes ES, Vink H, et al. (2009) Endothelial glycocalyx as potential diagnostic and therapeutic target in cardiovascular disease. Curr Opin Lipidol 20: 57-62.
16. Gil N, Goldberg R, Neuman T, Garsen M, Zcharia E, et al. (2012) Heparanase is essential

for the development of diabetic nephropathy in mice. Diabetes 61: 208-216.
17. Salmon AH, Ferguson JK, Burford JL, Gevorgyan H, Nakano D, et al. (2012) Loss of the endothelial glycocalyx links albuminuria and vascular dysfunction. J Am Soc Nephrol 23:1339-1350.
18. Smith ML, Long DS, Damiano ER, Ley K (2003) Near-wall micro-PIV reveals a hydrodynamically relevant endothelial surface layer in venules in vivo. Biophys J 85: 637-645.
19. Nieuwdorp M, van Haeften TW, Gouverneur MC, Mooij HL, van Lieshout MH, et al. (2006) Loss of endothelial glycocalyx during acute hyperglycemia coincides with endothelial dysfunction and coagulation activation in vivo. Diabetes 55: 480-486.
20. Nieuwdorp M, Meuwese MC, Mooij HL, Ince C, Broekhuizen LN, et al. (2008) Measuring endothelial glycocalyx dimensions in humans: a potential novel tool to monitor vascular vulnerability. J Appl Physiol 104: 845-852.
21. Martens RJ, Vink H, van Oostenbrugge RJ, Staals J (2013) Sublingual Microvascular Glycocalyx Dimensions in Lacunar Stroke Patients. Cerebrovasc Dis 35: 451-454.
22. Lambert J, Stehouwer CD (1996) Modulation of endothelium-dependent, flow-mediated dilatation of the brachial artery by sex and menstrual cycle. Circulation 94: 2319-2320.
23. Khairoun M, de Koning EJ, van den Berg BM, Lievers E, de Boer HC, et al. (2013) Microvascular damage in type 1 diabetic patients is reversed in the first year after simultaneous pancreas-kidney transplantation. Am J Transplant 13: 1272-1281.
24. Goedhart PT, Khalilzada M, Bezemer R, Merza J, Ince C (2007) Sidestream Dark Field (SDF) imaging: a novel stroboscopic LED ring-based imaging modality for clinical assessment of the microcirculation. Opt Express 15: 15101-15114.
25. Constantinescu A, Spaan JA, Arkenbout EK, Vink H, Vanteeffelen JW (2011) Degradation of the endothelial glycocalyx is associated with chylomicron leakage in mouse cremaster muscle microcirculation. Thromb Haemost 105: 790-801.
26. Vlahu CA, Lemkes BA, Struijk DG, Koopman MG, Krediet RT, et al. (2012) Damage of the Endothelial Glycocalyx in Dialysis Patients. Journal of the American Society of Nephrology.
27. Fiedler U, Reiss Y, Scharpfenecker M, Grunow V, Koidl S, et al. (2006) Angiopoietin-2 sensitizes endothelial cells to TNF-alpha and has a crucial role in the induction of inflammation. Nat Med 12: 235-239.
28. David S, Kumpers P, Hellpap J, Horn R, Leitolf H, et al. (2009) Angiopoietin 2 and cardiovascular disease in dialysis and kidney transplantation. Am J Kidney Dis 53: 770-778.
29. Khairoun M, van der Pol P, de Vries DK, Lievers E, Schlagwein N, et al. (2013) Renal ischemia/reperfusion induces a dysbalance of angiopoietins, accompanied by proliferation of pericytes and fibrosis. Am J Physiol Renal Physiol.
30. de Vries DK, Khairoun M, Lindeman JH, Bajema IM, de Heer E, et al. (2013) Renal Ischemia-Reperfusion Induces Release of Angiopoietin-2 From Human Grafts of Living and Deceased Donors. Transplantation.
31. Boehme MW, Deng Y, Raeth U, Bierhaus A, Ziegler R, et al. (1996) Release of thrombomodulin from endothelial cells by concerted action of TNF-alpha and

neutrophils: in vivo and in vitro studies. Immunology 87: 134-140.

32. Aso Y, Inukai T, Takemura Y (1998) Mechanisms of elevation of serum and urinary concentrations of soluble thrombomodulin in diabetic patients: possible application as a marker for vascular endothelial injury. Metabolism 47: 362-365.
33. Rehm M, Bruegger D, Christ F, Conzen P, Thiel M, et al. (2007) Shedding of the endothelial glycocalyx in patients undergoing major vascular surgery with global and regional ischemia. Circulation 116: 1896-1906.
34. Chappell D, Jacob M, Paul O, Rehm M, Welsch U, et al. (2009) The glycocalyx of the human umbilical vein endothelial cell: an impressive structure ex vivo but not in culture. Circ Res 104: 1313-1317.
35. Bartlett AH, Hayashida K, Park PW (2007) Molecular and cellular mechanisms of syndecans in tissue injury and inflammation. Mol Cells 24: 153-166.
36. Grundmann S, Fink K, Rabadzhieva L, Bourgeois N, Schwab T, et al. (2012) Perturbation of the endothelial glycocalyx in post cardiac arrest syndrome. Resuscitation 83: 715-720.
37. Sallisalmi M, Tenhunen J, Yang R, Oksala N, Pettila V (2012) Vascular adhesion protein-1 and syndecan-1 in septic shock. Acta Anaesthesiol Scand 56: 316-322.
38. Svennevig K, Kolset SO, Bangstad HJ (2006) Increased syndecan-1 in serum is related to early nephropathy in type 1 diabetes mellitus patients. Diabetologia 49: 2214-2216.
39. Nieuwdorp M, Mooij HL, Kroon J, Atasever B, Spaan JA, et al. (2006) Endothelial glycocalyx damage coincides with microalbuminuria in type 1 diabetes. Diabetes 55: 1127-1132.
40. Broekhuizen LN, Lemkes BA, Mooij HL, Meuwese MC, Verberne H, et al. (2010) Effect of sulodexide on endothelial glycocalyx and vascular permeability in patients with type 2 diabetes mellitus. Diabetologia 53: 2646-2655.
41. Martinez M, Vaya A, Alvarino J, Barbera JL, Ramos D, et al. (1999) Hemorheological alterations in patients with chronic renal failure. Effect of hemodialysis. Clin Hemorheol Microcirc 21: 1-6.


5